



# Novel Points of View for Endoscopy: Panoramized Intraluminal Opened Image and 3D Shape Reconstruction

Takuro Ishii<sup>1,\*</sup>, Satoki Zenbutsu<sup>2</sup>, Toshiya Nakaguchi<sup>3</sup>, Masashi Sekine<sup>2</sup>,  
Yukio Naya<sup>4</sup>, and Tatsuo Igarashi<sup>1</sup>

<sup>1</sup>Graduate School of Engineering, Chiba University, Inage ward,  
Chiba City, Chiba, 263-8522, Japan

<sup>2</sup>Research Center for Frontier Medical Engineering, Chiba University,  
Inage ward, Chiba City, Chiba, 263-8522, Japan

<sup>3</sup>Graduate School of Advanced Integrated Science, Chiba University,  
Inage ward, Chiba City, Chiba, 263-8522, Japan

<sup>4</sup>Teikyo University Chiba Medical Center, Ichihara City, Chiba, 299-0111, Japan

Endoscopic image of the tubular organs is recorded as discontinuous shots taken from a fixed angle without 3D or objective information. Presentation of a 3D picture of intraluminal cavity of the tubular organ covering whole-range of observation from continuous endoscopic video frames would be effective for the diagnosis and identification of the lesion, as well as offering intuitive information to the patients. In this paper, a new method for processing virtual endoscopy from "actual" endoscopic video images is proposed to observe the internal structures of tubular organs. The method consists of two steps of processing: 1. the panoramic image is processed from video image of endoscopy or the tubular organs where the endoscope was pulled at a constant speed automatically using a stepper motor or manually by a doctor. 2. the 3D-height information was extracted from a panoramic image using the intensity of the pixel based on the inverse-square law. This method is carried out under the assumption that the same part of the organ has similar property of reflection and the endoscope is the only source of illumination inside the body. The extracted height information will correspond with the distance between the point of the object and the endoscope. Finally, the virtual tubular object is reconstructed with the panoramic image texture. This method makes use of the advantages of conventional virtual endoscopy processed from "actual" endoscopic images, affording intuitive, multi-angle observation of the objects with color information and fine resolution. To date, virtual endoscopic images have been successfully processed from endoscopic video files for the colon, esophagus, ureter, and the urethra. Such images offer sharing of intuitive information for doctors and patients, and are promising in improving the accuracy of diagnosing the lesions.

**Keywords:** Endoscope, Medical Image Processing, Computer Graphics, Clinical Engineering, Virtual Endoscopy, Cystoscopy, Colonoscopy.

## 1. INTRODUCTION

Endoscopy is one of the most successful procedures in the modern clinical practice, designed to expand doctors' view into body cavities. Because the endoscope displays the color and shape of the objects, developmental trends in instrumentation and diagnosis include enhancement or attenuation of color information using fluorescence staining,<sup>1,2</sup> spectral analysis,<sup>3-6</sup> and demonstration of high-resolution images has been emerging. The recent development of robotic and laparoscopic surgery has created endoscopic vision known as the "surgeon's eye," along with video

processing that enables images to be shared among doctors and patients. In spite of additional advantages of the endoscope (e.g., ease of use, low cost, and simple structure), it sustains several disadvantages including the presence of blind corners, a narrow field of view, loss of perception of depth cue, and restricted motion that narrows the doctor's viewing angle. These drawbacks may reduce the sensitivity of endoscopy by interfering with recognition of information from the whole luminal cavity in deciding whether the endoscopic findings are pertinent in diagnosis, thereby affecting treatment planning and the treatment itself.

Various methods have been proposed to solve these spatial recognition problems in endoscopy. Recognition of depth cue can be achieved using binocular endoscopes, which have been

\*Author to whom correspondence should be addressed.

reported to be a useful tool for laparoscopic surgery under some restricted conditions.<sup>7-9</sup> Some investigations propose recognition of depth cue by movement parallax, using a monocular endoscope,<sup>10</sup> shape-from-shading method,<sup>11</sup> or by using an apparatus equipped with multi-lenses and charge coupled devices (CCDs). In assessing accurate shape, size or geometrical information of the lesion, previous techniques require large space enough to shake, push or pull the scope to cover whole area of the hollow organs. These operation is achieved in some limited conditions such as gastroenterology applied for the stomach. Widening of the field of view has been attempted by creating a panoramic image from camera motion<sup>12-14</sup> or using physical sensors; however, few of these approaches are acceptable for medical practice because of the limited volume of components and the requirements of safety, easy maneuverability, reliability of operation, and diagnostic accuracy. Thus, the drawbacks of the endoscope must be overcome, and the original appearance of the organs must be reproduced in a simple, easy, and accurate manner. From the next chapter, we introduce a novel view to show endoscopic video source for doctors and patients that contains color and approximated shape in wide-range of the interested organ, referring to the proposed method is adaptive to any endoscopic video imagery inserted to the tubular objects.

## 2. MATERIALS AND METHODS

### 2.1. Video Recording System

Conventional rigid and flexible endoscopes were used. Video signal was extracted from the S-video terminal of the video processor, and then connected to a computer via an A/D converter (Fig. 1). Endoscope is withdrawn inside of the interested tubular organ and recorded to a video file. In this method, one important concept is regarding endoscope as a scanner to produce a panoramic image. The fixed speed and axis make the result more better condition. Thus, a moving stage with a stepper motor is prepared to control endoscopic motion and used as possible. The workflow of the method is listed below:

- (1) Send the recorded endoscopic video signal to a PC as a digital video file (e.g., Audio Video Interleave (AVI)).
- (2) Create an opened panoramic image of the object from the video file.
- (3) Extract 3D information based on the luminance value of each pixel.

- (4) Fuse the 3D information (height value) with the values of 3D luminal coordinates.
- (5) The virtual tissue image created from the real video image is displayed on the PC monitor.

### 2.2. Opened Panoramic Image Processing

In processing an opened panoramic image of the tubular organs, we propose a novel setup: the object is determined as a cylindrical model, where the center of the axis of the virtual image is equal to the optical axis of the endoscope. Under these conditions, the luminal space of the tubular organs can be regarded as series of circles with two optional constant parameters: a center point and a radius. The video source is recorded while the operator pulls the scope straight through the luminal cavity. Optimal resolution is obtained by moving the endoscope slowly and at a constant pace so that a constant perspective is maintained along the axis of the luminal cavity. Color information for each pixel is acquired on a cursor circle set in each frame, and a one-dimensional array regarding color information on the circle is obtained as a fraction of the luminal cavity, assuming a cylindrical cavity. Continuous arrangement of the arrays for all frames between the in-out points of the movie provides an opened image of the luminal object. Figure 2 indicates relationship between a panoramic image and an input video imagery. In this processing, an output image formed with width of the same number of processed frames and height of  $2\pi r$ . Therefore, pixels in panoramic image  $P(u, v)$  are obtained from correspondent pixels in a video imagery using the following formula:

$$P(u, v) = V_u \left( r \sin \frac{v}{r} + c_x, r \cos \frac{v}{r} + c_y \right) \quad (1)$$

where  $V_t(x, y)$  indicate a pixel  $(x, y)$  in a frame  $t$  of the input video.  $r$ ,  $c_x$  and  $c_y$  indicate parameters of the designated circle, radius and a coordinate of the center point, respectively.

### 2.3. 3D Form Extraction

According to the inverse-square law for intensity, the relation between Luminance on the point of the object ( $L$ ) and distance ( $R$ ) from the light source is described as

$$L = a \frac{k_d \times I_q}{R^2} \cos \theta \quad (2)$$

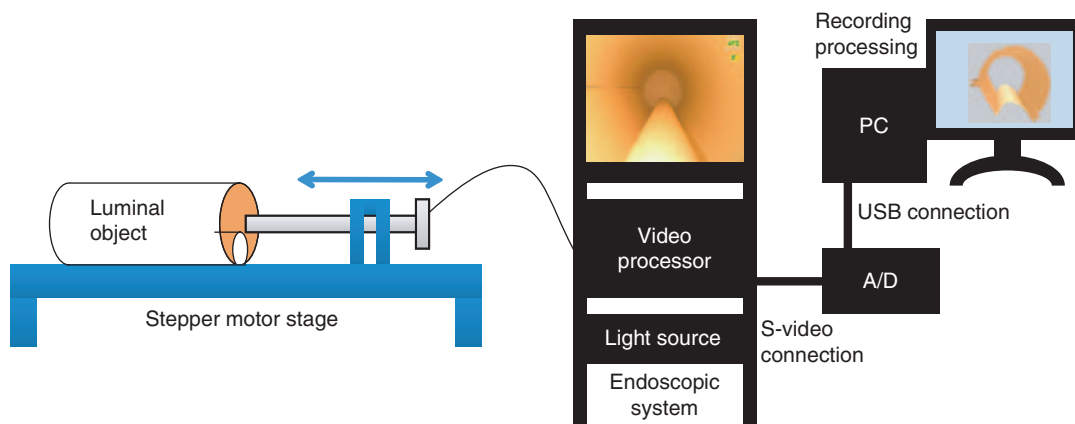


Fig. 1. Equipment system for recording and processing the endoscopic image.

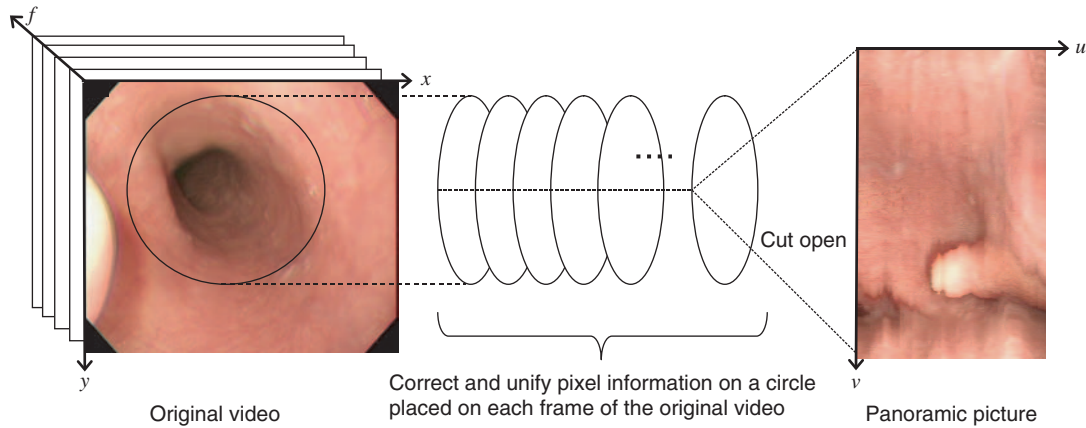


Fig. 2. Process followed in generating a panoramic image.

where  $k_d$  is the diffuse reflectance factor on the object’s surface,  $I_q$  is the intensity of the point light source,  $\theta$  is the angle of the incident ray, and  $a$  is a constant value. In this paper, The intensity of each pixel  $I(u, v)$  is regarded as that luminance value.

In this case, a single object in a living tissue approximates the reflection parameters processed from information of each pixel in a video image, under assumption that the diffusion from a light source are uniform on the cursor circle set on the video source during extracting information for the panorama image processing. These assumptions enable to set up  $k_d$  and  $I_q$  that are the constant value in the panoramic image. Since the incidence value  $\theta$  is almost impossible to obtain in a living object, it was expediently set as a constant value.

According to Eq. (2), the relative distance between the camera device and the point of the object is expressed as follows:

$$R(u, v) = k \sqrt{\frac{1}{I(u, v)^{(\gamma-1)}}} \quad (3)$$

where the  $R$  value expresses the relative value of the distance from the optical axis to the point correspond to a pixel  $u, v$  on the panoramic image.  $\gamma$  is one of proper parameter of the camera unit, and included to correct the linearity of the input intensity. This constant is measured with gray scale chart in advance.

Since the series of pixel on the circle is scanning the surface of the object along the endoscopic movement, the observed intensity for each pixel means the relational distance of the optical route (Fig. 3). Besides, owing to the optional circle parameter

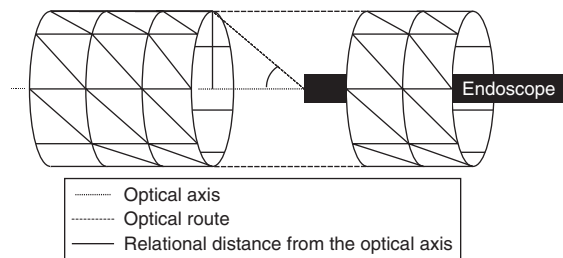


Fig. 3. Relation between the endoscope and the object. Both the 3D object and the panoramic image are divided into mesh units. Each vertex refers to color information from the pixel in the same position, and the relative distance is calculated between the optical axis and each point on the surface of the intraluminal cavity.

$(C_x, C_y, r)$  was fixed while processing a panoramic image, the included angle between optical axis and minimum optical route ( $\alpha$  in Fig. 3) is constant value in one processing. Therefore, the distance of the optical route may be regarded as the relational distance between optical axis and each point of surface.

### 2.4. Virtual Endoscopy Processed from Actual Endoscopic Imagery

Combination of the method described above for processing a panoramic image and calculation of the relative distance between the object and the scope enables depiction of opened panoramic and 3D images. Accordingly, this indicates the method for creating a virtual endoscopic image. Using the 3D form information, a series of distance values between the optical axis and the intraluminal of the object  $R(u, v)$ , the 3D coordinates,  $Out(X, Y, Z)$ , of a virtual object are determined as follows:

$$\begin{bmatrix} X \\ Y \\ Z \end{bmatrix} = w_1 R(u, v) \begin{bmatrix} \sin \omega \\ \cos \omega \\ 0 \end{bmatrix} + \begin{bmatrix} 0 \\ 0 \\ w_2 \cdot u \end{bmatrix} \quad (4)$$

$$\omega := 2\pi \frac{v}{H}$$

where  $H$  is the height size of the panoramic image, and  $w_1$  and  $w_2$  are optional values which are determined by experimental. Consequently, the final resolution of the constructed three-dimensional model is affected by some weight value, such  $k, w_1, w_2$ , which defined empirically.

A group of 3D points, indicated with Eq. (4), are processed to a group of polygons that build a 3D object in a virtual space. Finally, the panoramic image covers the object as a texture to complete virtual endoscopic view.

## 3. EXPERIMENTS AND RESULTS

### 3.1. Simulated “Dummy” Model to Approximate the Colon

Prior to *in vivo* experiments, we tested the accuracy of the processed images using three simple models. The first model was a simple polyvinyl chloride pipe with a diameter of 4 cm. A light orange-colored cylindrical stick (1 cm in diameter) was placed as an object inside the pipe, the inner cavity of which was covered with the paper of the same color. Another hemispherical

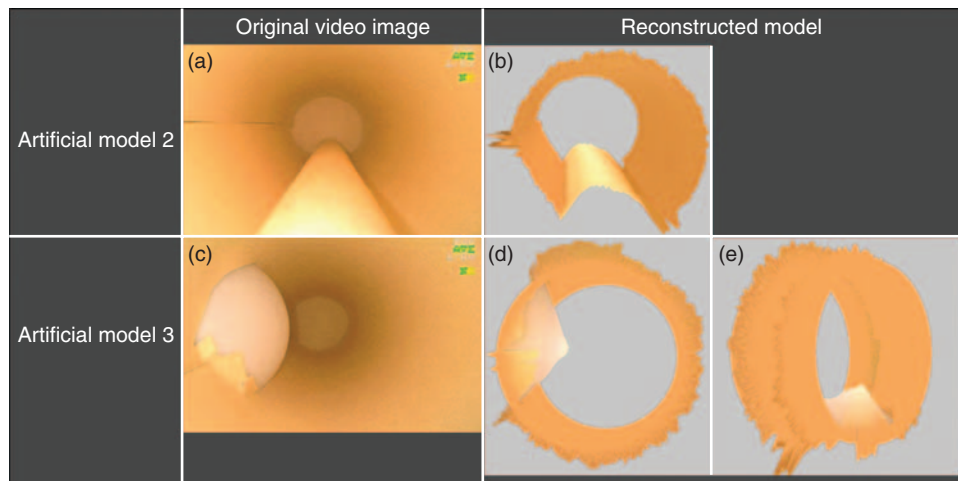


**Fig. 4.** Results obtained using the “dummy” model. (a) Input video image of artificial model 2 (a simple pipe with a stick placed inside). (b) Processed image from video “a”. (c) Input video image of artificial model 3 (a pipe with a half-sphere placed inside). (d) Processed image from video “c”. Specular reflection of the original image has made the top of the sphere appear sharp. (e) Image of processed model “d”, displayed from the opposite side. The opposite side of the sphere resembles a cliff because the input video retrieves no information from its blind corner.

object was placed inside the pipe through a hole in the wall of the pipe. As shown in Figure 1, a rigid laparoscope (10 mm in diameter), mounted on a moving stage and controlled at a speed of 1 cm/sec with a fixed axis, was inserted into the pipe, and its video image was recorded during withdrawal of the scope. To evaluate the resolution for the small lesion in the panoramic image, some 1 mm square rectangles arranged at 3 mm intervals on a paper, set inside a pipe, was used. The video image was recorded using a rigid laparoscope fixed on a stepper motor with the controlled velocity and optical axis, and the video image is captured at 30 fps.

### 3.2. Verification *In Vivo*

We tested the image processing method using porcine colon. The experiment was performed under the approval of the local Ethics Committee for Animal Experiments. Endoscopy was performed on a pig weighing 30 kg, under general anesthesia by inhalation of halothane and sevoflurane. The entire colon was resected and extracted. After washing out the luminal cavity, the oral end was ligated and was expanded insufflations with air. A rigid laparoscope (10 mm in diameter) was then inserted from the anal end and a video image was recorded during withdrawal at a speed of 1 cm per second.

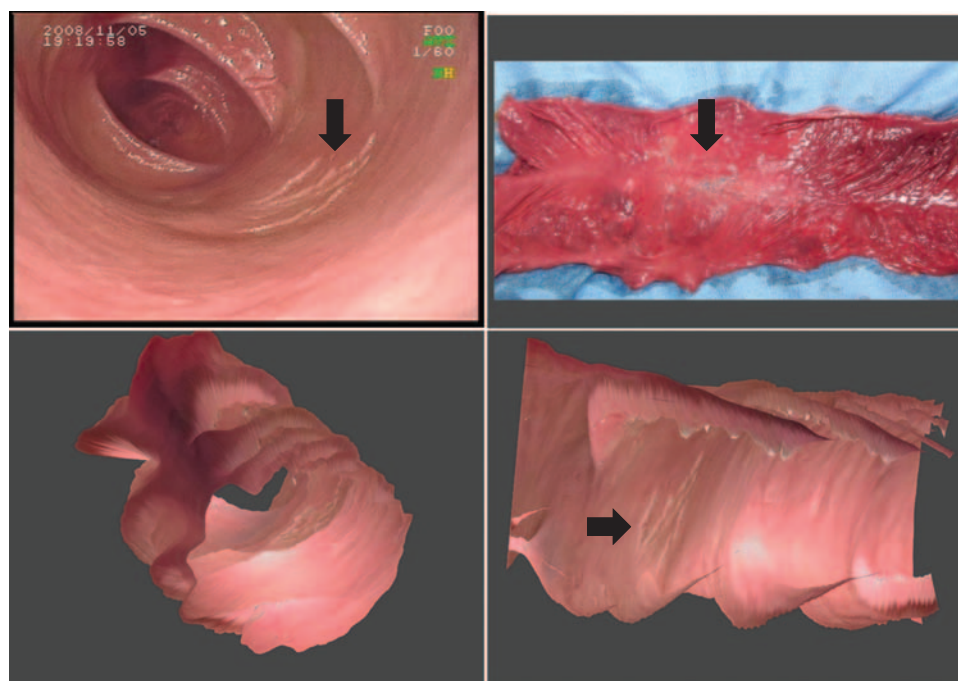


**Fig. 5.** Trial using porcine colon. Arrows indicate *torn lesion*.

In the next step, video files of human endoscopy were tested, with approval from the local Ethics Committee for Research using Human Specimens, and with the informed consent of patients. Between January 2008 and March 2009, video files were recorded during routine clinical practice in five patients after colonoscopy and in three patients after gastroduodenoscopy; in three patients with ureteral calculus scheduled for transurethral ureterolithotripsy; and in five patients with benign prostate hyperplasia just before transurethral resection of prostate. The procedures were performed at Chiba University Hospital and two other hospitals. The endoscope was slowly pulled through the lumen by the operator while the video files were being recorded.

In all trials of the above three models, panoramic images could be processed automatically. Optimal velocity of pulling the endoscope was found to be below 25 mm/sec to acquire clear depiction of 1 mm sized square in case of 30 fps. Blurring was observed when the endoscope pulled faster than 25 mm/sec that surely related to overlook of the fine lesions. In the virtual endoscopic trial using a pipe with a stick placed inside, reconstruction of the 3D shape of the pipe and the upper half of the surface of the stick was achieved with satisfactory consistency, except

for the lower half of the stick, which could not be depicted (Figs. 4(a, b)). Because the video images are a projection, the blind corner of the stick and the shade around it interrupts the extraction of accurate brightness information in each pixel when the original shape is recovered.

For the model trial using a pipe and a sphere (Figs. 4(c–e)), the far side of the sphere was depicted as a “cliff” because of the blind corner that occurred in endoscopic observation. Furthermore, pixels exposed to excessive illumination displayed halation when the tip of the endoscope passed very close to the top of the sphere, causing a steep increase in the value of brightness. In this situation, a sharp conformation appears in the virtual object.

In the trial using porcine colon, panoramic processing ran automatically, with moderate consistency (Fig. 5). The virtual endoscopic image processed by our method showed some spikes on its conformation, which was caused by specular reflection on the point of the real object. In contrast, it is noteworthy that torn lesions on the surface could be confirmed on the virtual object. The trial verified that the resolution of the image on the generated object is sufficient for medical applications.

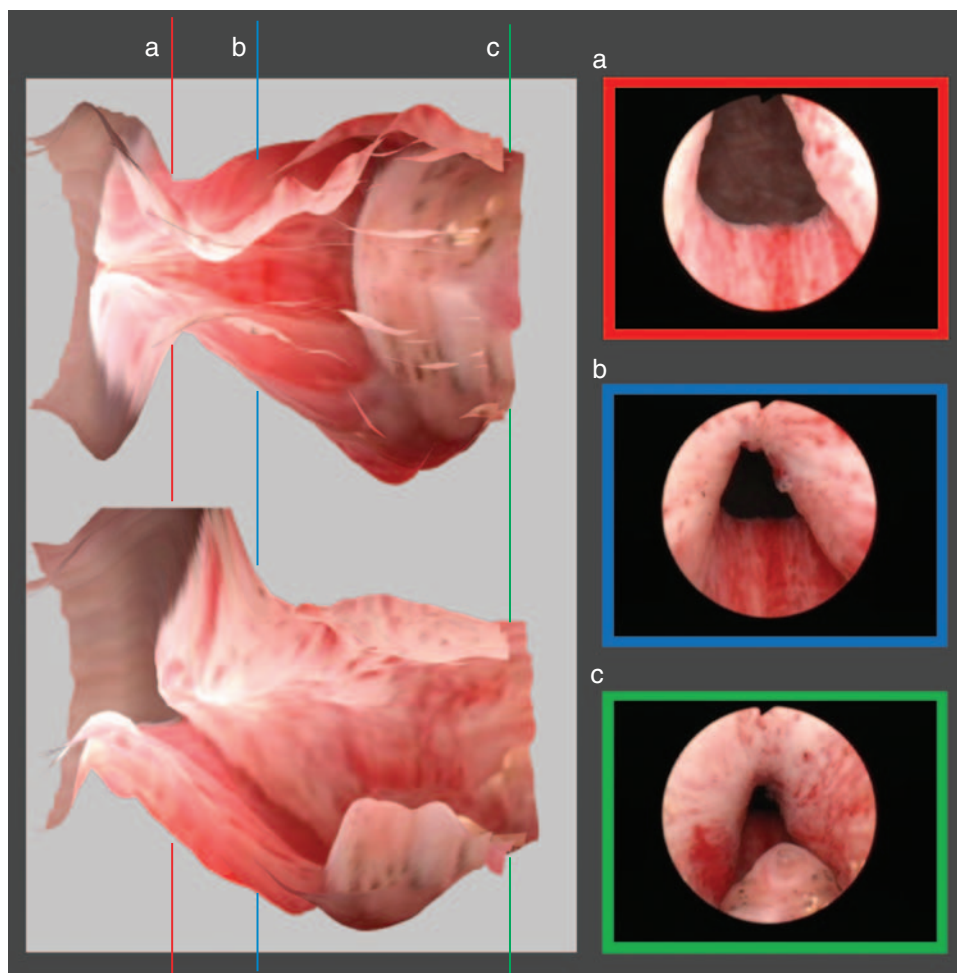


**Fig. 6.** Resultant images of the human male urethra. The two images on the left show sections of the reconstructed 3D virtual models. Top image, superior view from the top to the bottom of the model; bottom image, view of the right interior side from the contralateral side. The colored lines correspond to the endoscopic pictures of the same colors that are shown on the right. The left side of the virtual image corresponds with the entrance to the bladder, continuing to the right toward the urethral opening.

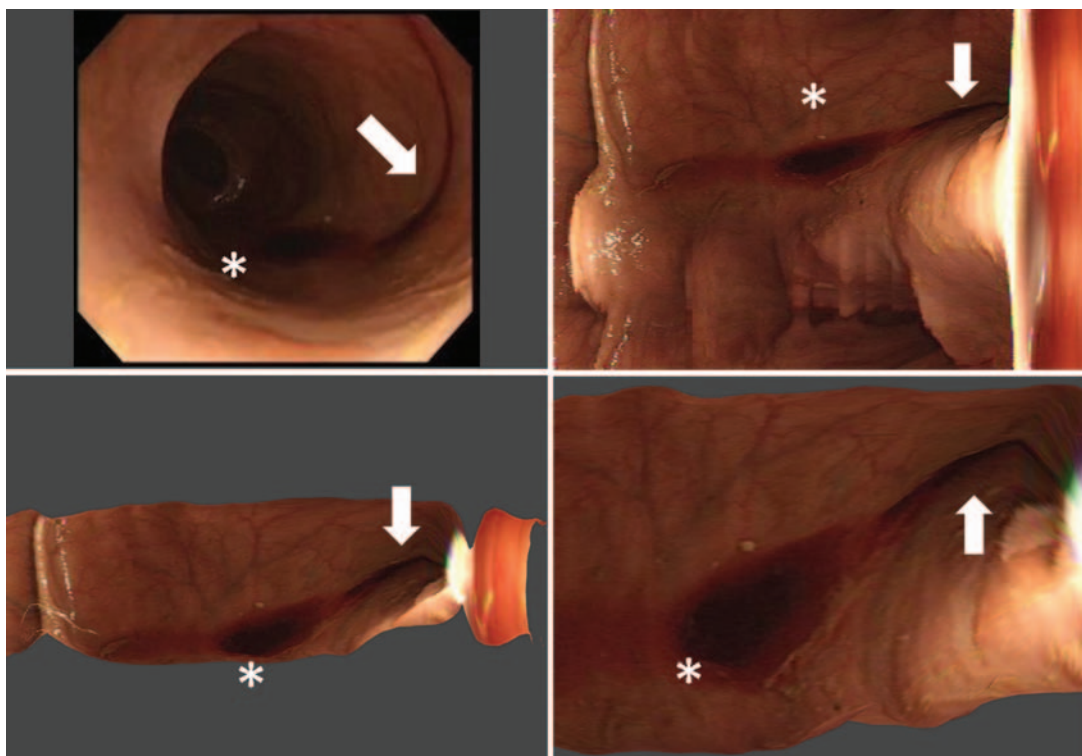


**Fig. 7.** Resultant images of the human colon. Arrows: flood of bleeding from an unknown site. Asterisks: blood pool.

The trial that used video files of the human male urethra, recorded during transurethral resection of the prostate or bladder cancer, revealed more complex structures when compared with the above artificial model and the porcine colon. Panoramic imaging clearly depicted structures in detail, including patterns of fine vessels and protrusion of the prostate. The generated virtual 3D model also depicted structures clearly, with findings consistent with those of MRI and urethrography in terms of observing the condition of the lower urinary tract (Fig. 6). This result indicates that the cystoscope stretched the tissue, causing the blind corner to disappear. Figure 7 reveals opened panoramic and virtual image of the human colon processed from conventional colonoscopy for patients showing bleeding front the alimentary tracts. Flood of Bleeding can be observed from multiple angles enabling to trace the site of lesion (not shown in the figure), indicating clinical relevancy of observing and recording the intraluminal space objectively to reach accurate diagnosis.

#### 4. DISCUSSION

The rapid improvement in computer processor performance in the past decade has enabled 3D reconstruction of CT and MRI data, which can be achieved even by a personal laptop computer equipped with the appropriate software. Such advances in computer technology have gained acceptance among engineers and doctors,<sup>15</sup> and motivated the further development of new medical tools. Virtual endoscopy processed from digital imaging and communication in medicine (DICOM) data of CT or MRI has recently gained wide acceptance,<sup>16</sup> as it enables observation of lesions from multi-angle viewpoints with sequential information and is reported to be less invasive than conventional endoscopy,<sup>17–20</sup> enhancing diagnostic sensitivity in some organs.<sup>21,22</sup> In other

words, with improvement of resolution, together with the use of adequate contrast medium, virtual endoscopy can be applied to most of the tubular organs, with advantages of cancellation of the blind spot, free control of view points, and less invasiveness compared with conventional endoscopy. The resolution of virtual endoscopy is dependent on that of the original image obtained from imaging apparatus; therefore, the resolution of currently available multidetector CT enables imaging resolution comparable to that of conventional endoscopy in detecting lesions under 5 mm in size in the urinary bladder.<sup>23</sup> CT and MRI images, however, contain no color information, making lesion detection reliant on the spatial resolution of the sequential information. On the other hand, the “actual” endoscope provides color information with fine resolution, to some extent. Thus virtual endoscopy processed from the “actual” endoscopic image also would have potential to depict structure in detail and may offer a solution to the drawbacks of “actual” endoscopy. Therefore, the fusion of high-resolution color information, extracted from “actual” endoscopy, with a virtual endoscopic image would offer more intuitive information to patients and doctors, and would be expected to raise the sensitivity of lesion diagnosis.

Various methods have been proposed to achieve this aim. Hakamada et al.<sup>24</sup> attached magnetic sensors to the port for insertion of the scope and monitoring of its position and angle. However, their method regarded organs as rigid bodies, resulting in inconsistencies between the CT and endoscopic images with regard to shape and position of the soft and elastic organs.

Direct extraction of organ information from actual endoscopic images is a clue to solving this problem. Because conventional monocular endoscopy is equipped with only one CCD unit, advanced methods have been attempted to extract 3D information of lesions, by endoscopic profilometry using slit beam projection<sup>25</sup> or by adapting the shape-from-shading method.<sup>11</sup>

Another underlying problem of endoscopy is that magnified images are obtained at the expense of a wide field of view. Accordingly, reconstruction of the spatial structure of the whole luminal cavity, as observed by endoscopy, is reliant on the doctor's ability, or necessitates the recording of a large number of images. Recent reports propose the processing of a panoramic image from endoscopic video data using image mosaicing technology that calculates the mutual relationship between the object and the endoscope, and position and axis along the center of the tubular object, and projects the image around the axis.<sup>13,14</sup> Such trials appear to have promise for recording and filing endoscopic findings; however, motion of both the object in the luminal cavity and the endoscope is generally so rapid that it is difficult to process a continuous, panoramic image in an automated manner. We propose a different method that uses a simple algorithm to process a panoramic picture of the luminal cavity from endoscopic video images containing 3D information, providing a map of the luminal cavity that enables an understanding of spatial relationships between anatomical tissue landmarks and lesions.

The resolution of the processed image is determined by several system parameters; resolution and frame rate of original video images, the velocity of endoscope, and the optional radius set on the each video frame to extract information for panoramic image production. Under the experimental environments, such as fixed axis and velocity of endoscope movement, it's natural that the resolution is simply dependent on the velocity of endoscopic motion. This experiment and other processed image (such as shown in Figs. 5 and 7) demonstrate that the sequence of panoramic image processing represent intimate information of the intra-luminal object under appropriate speed of endoscope. This panoramic image is effective to grasp the distribution of the structures and lesions roughly on the surface of the lumen. However, the velocity is also operative to change the size for the direction of depth. The method to correct the distortion for the depth axis will be introduced in the next step.

In turn, this method can generate a virtual 3D model containing actual color texture as well as shape information in a completely different method of processing shape reconstruction from CT or MRI.

We proposed a method for virtual endoscopy in which an axis (set as the track of the endoscope passing through the center of the optical axis) was used to calculate the relative distance between the object and the tip of the endoscope according to pixel brightness, at a fixed angle to the optical axis. One drawback of the method is specular reflection on the surface of the organ, which interferes with extraction of the true brightness values in calculating the relative distance. Thus, reconstruction of the architecture of intraluminal objects becomes crude. Because we assumed the object to be a straight cylinder, it will not always fit the bent portions of some organs, such as bends in the colon. Another problem is attributable to the properties of the endoscope: blind corners will always exist during observation. This information gap results in skewing of the form of the structure. Measurement of the absolute distance between the endoscope and the object, and monitoring of endoscope motion, would require additional attachments; however, this appears impractical because detection of the lesion is a propriety matter. Our method produces an opened panoramic image, a 3D shape approximating the original one, and virtual endoscopic images, none of which are obtained in conventional endoscopy; the method also enables

mapping of the luminal cavity and comparison of the size of lesions.

One of the prominent advantages of virtual endoscopy is that it provides patients and doctors with intuitive animated images with multi-angle observation, and a flattened image of the whole area of the organ.<sup>26</sup> In other words, virtual endoscopy is a potent tool that will enable patients and doctors to share information and obtain consensus. Despite the problems that remain, displaying a virtual image of the "actual" endoscopic image facilitates observation of the entire pathway of the luminal cavity and the location of lesions from multi-angle viewpoints.

## 5. FUTURE DEVELOPMENTS

Color attenuation using filters and illumination<sup>27,28</sup> and specific software<sup>5,6</sup> is an effective method for endoscopic lesion detection that requires no additional equipment. The combination of a color-attenuating endoscope and fluorescence method<sup>2,29,30</sup> with the proposed method appears an attractive method of displaying the virtual endoscopic image, while enhancing non-protuberant lesions such as dysplasia or malignant disease with infiltrating potential. Although some problems remain, the present study indicates that generation of the 3D structure of the channel of particular organs is feasible using conventional endoscopes. This means that a fluid dynamic model, relevant to the pathological condition of organs with high-speed fluid within the luminal cavity such as the upper airway, coronary artery, and lower urinary tract, could be created from an endoscopically recorded video image. Among these organs, CT and MRI fail to extract information unless voiding of contrast media is performed during scanning.<sup>31,32</sup> In this respect, endoscopy is superior to CT and MRI in simulating transformation of the channel under water pressure by irrigation. The mechanism of voiding dysfunction remains indistinct. A previous study hypothesizes that voiding dysfunction is related to angulation of the prostatic urethra<sup>33</sup> or to the loss of hydraulic energy in the urine flow during passage through the urethra.<sup>34</sup> The present study has the potential to offer insight into these hypotheses.

Several studies report virtual endoscopy of the coronary arteries, processed from CT.<sup>19,35</sup> However, it is important that plaque is colored to predict the future occurrence of ischemic heart attack. Because vascular endoscopy is carried out under saline irrigation, the proposed method could be adapted to process a virtual endoscopic image with color information that indicates the location of abnormal plaque.

## 6. CONCLUSIONS

We proposed a method for processing a virtual endoscopic view obtained from conventional "actual" endoscopic video files. The technical aspects of the method are summarized as follows:

1. The conventional endoscope is used as a scanner, and is pulled through the luminal cavity at a constant speed and perspective view;
2. A panoramic image of the object is processed, assuming that the structure of the object approximates a cylinder;
3. 3D conformation is extracted on the surface, based on the inverse-square law and the correction to utilize the luminance value of each pixel on a panoramic image; and

4. A virtual 3D model of the object is produced that has both color and 3D shape information by combining the cylindrical approximation with the extracted configuration data.

Despite problems that interfere with accurate processing of the shape of the original structure, the intuitive character of the resultant image enables detection and identification of lesion location. We conclude that virtual endoscopic images processed from “actual” endoscopic video images are a new and challenging modality, and may be complimentary to those processed from CT or MRI image data.

## References and Notes

1. T. Wang, J. Van Dam, J. Crawford, E. Preisinger, Y. Wang, and M. Feld, *Gastroenterol.* 111, 1182 (1996).
2. M. Mehlmann, C. S. Betz, H. Stepp, S. Arbogast, R. Baumgartner, G. Grevers, and A. Leunig, *Lasers Surg. Med.* 25, 414 (1999).
3. H. Zeng, M. Petek, J. Dao, B. Palcic, and G. Ferguson, Automated endoscopy device, diagnostic method and uses, US Patent US2005/0059894 A1, March (2005).
4. K. Kuznetsov, R. Lambert, and J. F. Rey, *Endoscopy* 38, 76 (2006).
5. J. Pohl, M. Nguyen-Tat, O. Pech, A. May, T. Rabenstein, and C. Ell, *Am. J. Gastroenterol.* 103, 562 (2008).
6. Y. X. Liu, L. Y. Huang, X. P. Bian, J. Cui, N. Xu, and C. R. Wu, *Chin. Med. J. (Engl)* 121, 977 (2008).
7. E.M. McDougall, J. J. Soble, J. Stuart Wolf, Jr., S. Y. Nakada, O. M. Elashry, and R. V. Clayman, *J. Endourol.* 10, 371 (1996).
8. N. Taffinder, S. G. Smith, J. Huber, R. C. G. Russell, and A. Darzi, *Surg. Endosc.* 13, 1087 (1999).
9. C. C. Sun, A. W. Chiu, K. K. Chen, and L. S. Chang, *Urol Int.* 64, 154 (2000).
10. F. A. Voorhorst, K. J. Overbeeke, and G. J. F. Smets, *Med. Prog. Technol.* 21, 211 (1996).
11. K. Deguchi and T. Okatani, *Computer Vision and Image Understanding* 66, 119 (1997).
12. S. Peleg and J. Herman, Panoramic mosaic with VideoBrush, *DARPA Image Understanding Workshop* (1997), p. 255.
13. R. Miranda-Luna, C. Daul, W. C. P. M. Blondel, Y. Hernandez-Mier, D. Wolf, and F. Guillemain, *IEEE Trans. Biomed. Eng.* 55, 541 (2008).
14. E. J. Seibel, R. E. Carroll, J. A. Dominitz, R. S. Johnston, C. D. Melville, C. M. Lee, S. M. Seitz, and M. B. Kimmey, *IEEE Trans. Biomed. Eng.* 55, 1032 (2008).
15. K. Nakamura, Y. Naya, S. Zenbutsu, K. Araki, S. Cho, S. Ohta, N. Nihei, H. Suzuki, T. Ichikawa, and T. Igarashi, *J. Endourol.* 24, 521 (2010).
16. R. M. Satava, *Surg. Endosc.* 10, 173 (1996).
17. S. Okimasa, S. Shibata, Y. Awaya, Y. Nagao, I. Murakami, and E. Shigeto, *Respirol.* 12, 607 (2007).
18. S. Men, M. C. Ecevit, I. Topcu, N. Kabacki, T. K. Erdag, and S. Sutay, *J. Digit. Imaging* 20, 67 (2007).
19. P. M. A. van Ooijen, G. de Jonge, and M. Oudkerk, *Eur Radiol.* 17, 2852 (2007).
20. G. Battista, C. Sassi, R. Schiavina, A. Franceschelli, E. Baglivo, G. Martorana, and R. Canini, *Abdom Imaging* 34, 107 (2008).
21. S. K. Kim, J. M. Lee, H. W. Eun, M. W. Lee, J. K. Han, J. Y. Lee, and B. I. Choi, *Radiol.* 244, 852 (2007).
22. S. Croitoru, B. Moskovitz, O. Nativ, E. Barmer, and N. Hiller, *Abdom Imaging* 33, 717 (2008).
23. C. Tsampoulas, A. C. Tsili, D. Giannakis, Y. Alamanos, N. Sofikitis, and S. C. Efremidis, *Am. J. Roentgenol.* 190, 729 (2008).
24. S. Hakamada, D. Miyoshi, T. Nakaguchi, T. Tsumura, and Y. Miyake, *IEICE Technical Report* 105, 13 (2006).
25. H. Haneishi, T. Ogura, and Y. Miyake, *Optics Lett.* 19, 601 (1994).
26. S. Haker, S. Angenent, A. Tannenbaum, and R. Kikinis, *IEEE Trans. Med. Imaging* 19, 665 (2000).
27. R. Lambert, K. Kuznetsov, and J. F. Rey, *Scientific World Journal* 7, 449 (2007).
28. F. Emura, Y. Saito, and H. Ikematsu, *World J. Gastroenterol.* 14, 4867 (2008).
29. T. D. Wang, J. Crawford, M. Feld, Y. Wang, I. Itzkan, and J. V. Dam, *Gastrointest Endosc.* 49, 447 (1999).
30. M. A. Kara and J. J. Bergman, *Endoscopy* 38, 627 (2006).
31. C. P. Chou, J. S. Huang, M. T. Wu, H. B. Pan, F. D. Huang, C. C. Yu, and C. F. Yang, *AJR Am. J. Roentgenol.* 184, 1882 (2005).
32. E. Yekeler, E. Suleyman, A. Tunaci, N. Balci, K. Onem, M. Tunc, and G. Acunas, *Magn. Reson. Imaging* 22, 1193 (2004).
33. K. S. Cho, *Med. Hypotheses* 70, 532 (2008).
34. M. Tojo, K. Yasuda, T. Yamanishi, T. Hattori, K. Nagashima, and J. Shimazu, *J. Urol.* 152, 144 (1994).
35. T. Nakanishi, M. Kohata, K. Miyasaka, H. Fukuoka, K. Ito, and M. Imazu, *AJR Am. J. Roentgenol.* 174, 1345 (2000).

Received: 6 July 2010. Revised/Accepted: 18 September 2010.